Supplementary material: Impact of Time-History Terms on Reservoir Dynamics and Prediction Accuracy in Echo State Networks

Yudai Ebato[1*], Sou Nobukawa[1,2,3], Yusuke Sakemi[4,8], Haruhiko Nishimura[5], Takashi Kanamaru[6], Nina Sviridova[7,8], Kazuyuki Aihara[4,8]

[1*]Graduate School of Information and Computer Science, Chiba Institute of Technology, 2-17-1 Tsudanuma, Narashino, 275–0016, Chiba, Japan.
[2]Department of Computer Science, Chiba Institute of Technology, 2-17-1 Tsudanuma, Narashino, 275–0016, Chiba, Japan.
[3]Department of Preventive Intervention for Psychiatric Disorders, National Center of Neurology and Psychiatry, 4-1-1 Ogawa-Higashi, Kodaira, 187–8551, Tokyo, Japan.
[4]Research Center for Mathematical Engineering, Chiba Institute of Technology, 2-17-1 Tsudanuma, Narashino, 275–0016, Chiba, Japan.
[5]Faculty of Informatics, Yamato University, 2-5-1 Katanama chou, Suita, 564–0082, Osaka, Japan.
[6]Department of Mechanical Science and Engineering, School of Advanced Engineering, Kogakuin University, 192–0015 Tsudanuma, Hachioji, 275–0016, Tokyo, Japan.
[7]Department of Intelligent Systems, Tokyo City University, 1 choume 28-1 Tamatsuzumi, Setagaya, 158–8557, Tokyo, Japan.
[8]International Research Center for Neurointelligence, The University of Tokyo Institutes for Advanced Study, The University of Tokyo, 7 choume 3-1 Hongou, Bunkyou ku, 113-8654, Tokyo, Japan.

*Corresponding author(s). E-mail(s): s1831701fj@s.chibakoudai.jp;
Contributing authors: nobukawa@cs.it-chiba.ac.jp; yusuke.sakemi@p.chibakoudai.jp; nishimura.haruhiko@yamato-u.ac.jp; kanamaru@cc.kogakuin.ac.jp; nina@tcu.ac.jp; kaihara@g.ecc.u-tokyo.ac.jp;

1 Analysis of maximum Lyapunov exponent

1.1 Maximum Lyapunov exponent

The maximum Lyapunov exponent λ serves as a metric for measuring orbital instability in dynamical systems [1]. This metric is obtained through several equations, which can vary depending on the system under consideration. For a fully-leaky Echo State Network (ESN)/Leaky-Integrator ESNs (LI-ESN), the reference orbit $\mathbf{s}_k(t)$ is defined as:

$$\mathbf{s}_k(t_0) = \mathbf{x}(T_b + \tau k). \tag{S1}$$

In the case of Chaotic Echo State Networks (ChESN), the system possesses three internal states $\boldsymbol{\xi}(t)$, $\boldsymbol{\eta}(t)$, and $\boldsymbol{\zeta}(t)$, and the reference orbit is given by:

$$\mathbf{s}_k(t_0) = \begin{bmatrix} \boldsymbol{\xi}(T_b + \tau k) \\ \boldsymbol{\eta}(T_b + \tau k) \\ \boldsymbol{\zeta}(T_b + \tau k). \end{bmatrix}. \tag{S2}$$

For each initial condition, the perturbed orbit $\mathbf{s}'_k$ evolves over a time period τ, with t_l indicating the time evolution of the perturbation. It starts from an initial condition obtained by adding a perturbation $\boldsymbol{\delta}_k^{(t_l=0)}$ to the reference orbit $\mathbf{s}_k(t)$:

$$\mathbf{s}'_k(t_0) = \mathbf{s}_k(t_0) + \boldsymbol{\delta}_k^{(t_l=0)}. \tag{S3}$$

The difference between the perturbed and reference orbits after the time evolution, denoted by $\boldsymbol{\delta}_k^{(t_l=\tau)}$, is calculated:

$$\boldsymbol{\delta}_k^{(t_l=\tau)} = \mathbf{s}'_k(t_0 + \tau) - \mathbf{s}_k(t_0 + \tau). \tag{S4}$$

For $k > 1$, this initial perturbation is computed using:

$$\boldsymbol{\delta}_k^{(t_l=0)} = \frac{|\boldsymbol{\delta}_1^{(t_l=0)}|}{|\boldsymbol{\delta}_{k-1}^{(t_l=\tau)}|} \boldsymbol{\delta}_{k-1}^{(t_l=\tau)}. \tag{S5}$$

Here, the first perturbation vector $\boldsymbol{\delta}_1^{(t_l=0)}$ is a vector of ones ($\mathbf{1} = [1, 1, \ldots, 1]^T$) scaled to a small value $|\boldsymbol{\delta}_1^{(t_l=0)}| = \delta_0 = 10^{-5}$:

$$\boldsymbol{\delta}_1^{(t_l=0)} = \delta_0 \frac{\mathbf{1}}{|\mathbf{1}|} \tag{S6}$$

The Lyapunov exponent λ_k for each initial condition is determined based on the growth of this perturbation:

$$\lambda_k = \frac{1}{\tau} \ln \frac{|\boldsymbol{\delta}_k^{(t_l=\tau)}|}{|\boldsymbol{\delta}_k^{(t_l=0)}|}. \tag{S7}$$

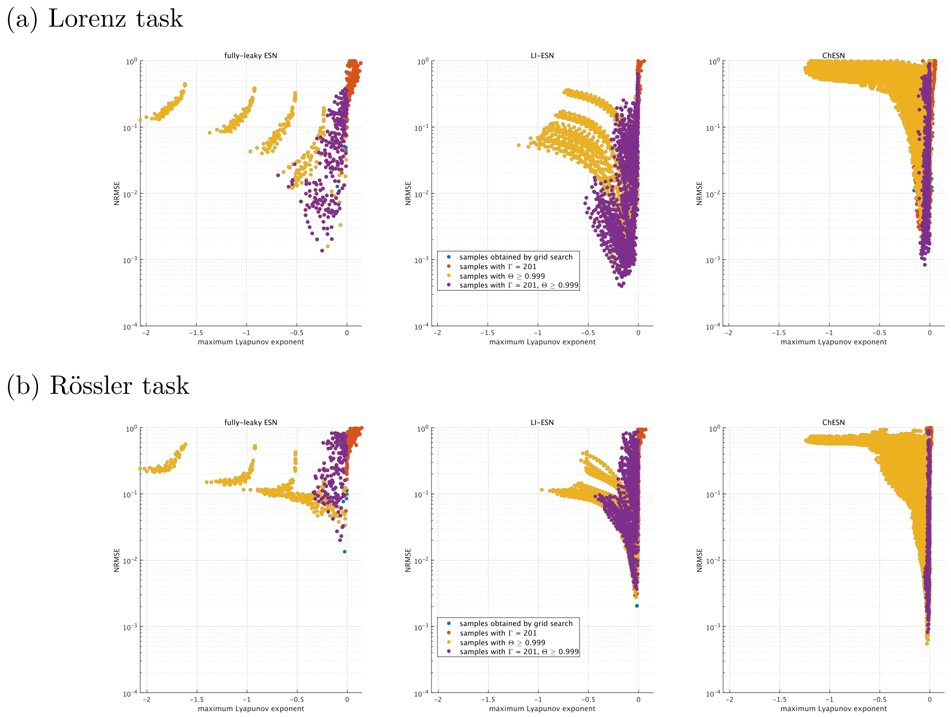

Fig. S1 Correspondence between time-series prediction performance and maximum Lyapunov exponents. This scatter plot illustrates the relationship between the normalized root mean square error (NRMSE) and memory capacity in time-series prediction tasks for both the Lorenz and Rössler systems. Each point on the scatter plot originates from grid search results, which include the optimal parameters as obtained in Fig. 5 in a main text. Grid search parameters are shown in Table. 1 in a main text.

Finally, λ is computed by averaging these λ_k values over all K different initial conditions:

$$\lambda = \frac{1}{K}\sum_{k=1}^{K}\lambda_k. \tag{S8}$$

This overall process gives us a measure of the system's sensitivity to initial conditions by capturing the degree of development of the perturbation over time.

1.2 Scatter plot of the maximum Lyapunov exponent and performance

Figure S1 displays a plot of the maximum Lyapunov exponent. This figure clearly shows that the highest performance occurs when the maximum Lyapunov exponent is near zero, indicating the edge of stability [2]. Additionally, consistency typically achieves its maximum value when the Lyapunov exponent is zero or negative. Moreover, the covariance rank tends to be maximized when the maximum Lyapunov exponent is near zero or larger. Notably, at the edge of stability, where the reservoir's performance is optimized, both the covariance rank and consistency are observed to reach their maximum values.

The maximum Lyapunov exponent is an indicator for evaluating the chaotic characteristic of dynamics, and a system with $\lambda > 0$ exhibits chaotic state [1]. From the perspective of reservoir computing, the maximum Lyapunov exponent has been used as an index to identify the reservoir dynamics where performance is optimized [2]. The diversity of reservoir dynamics tends to be higher when the maximum Lyapunov exponent is high; however, performance degrades when the Lyapunov exponent exceeds a certain threshold, as the reservoir stability is compromised (i.e., the consistency between the input and output signals is not maintained). Therefore, optimal reservoir dynamics tend to be achieved at high maximum Lyapunov exponents, up to the point just before the stability of the reservoir is lost $\lambda \approx 0$. This point is commonly referred to as the"edge of chaos," but, Carroll argues that the term "edge of stability" is more appropriate in the context of reservoir computing, as the essential dynamic characteristic is not the system's chaotic nature, but rather the consistency between its input and output signals (echo state property) [2].

Furthermore, achieving optimal performance is not solely dependent on the diversity and stability of the reservoir. Carroll's experiments indicate that the edge of stability does not necessarily correspond to optimal performance, suggesting that there may be other dynamic characteristics that need to be simultaneously fulfilled to achieve optimal performance [2]. According to this finding, in this study, we focus on memory, which is likely related to time-history terms among such performance-related dynamic characteristics.

Moreover, it is not possible to gauge the level of stability and diversity of reservoir dynamics solely from the maximum Lyapunov exponent. In the main text, we introduce metrics for independently measuring dynamic diversity and stability, namely covariance rank [3] and consistency[4, 5], as we need to compare the reservoir dynamics of fully-leaky ESN, LI-ESN, ChESN.

2 The correspondence of simplified ChESN and LI-ESN.

We compare the performance of a simplified version of ChESN (simple-ChESN) with LI-ESN. The reservoir update equation for simple-ChESN is derived from Eq. (4) in the main text, setting all decay coefficients to a common value ($k = k_e = k_f = k_r$) and scaling the refractory parameter α and threshold θ to zero:

$$\begin{aligned}\mathbf{x}(t+1) &= \tanh(\boldsymbol{\xi}(t+1) + \boldsymbol{\eta}(t+1) + \boldsymbol{\zeta}(t+1)),\\ \mathbf{x}(t+1) &= \tanh(k(\boldsymbol{\xi}(t) + \boldsymbol{\eta}(t) + \boldsymbol{\zeta}(t)) + \mathbf{W}_{\text{in}}\mathbf{u}(t+1) + \mathbf{W}\mathbf{x}(t)).\end{aligned} \tag{S9}$$

Here, by denoting the internal state of the chaotic neuron as $\mathbf{y_{ch}}(t) = \boldsymbol{\xi}(t)+\boldsymbol{\eta}(t)+\boldsymbol{\zeta}(t)$, Eq. S9 can be simply expressed as:

$$\begin{aligned}\mathbf{x}(t+1) &= \tanh(\mathbf{y_{ch}}(t+1)),\\ \mathbf{x}(t+1) &= \tanh(k\mathbf{y_{ch}}(t) + \mathbf{W}_{\text{in}}\mathbf{u}(t+1) + \mathbf{W}\mathbf{x}(t)).\end{aligned} \tag{S10}$$

(a) Lorenz task

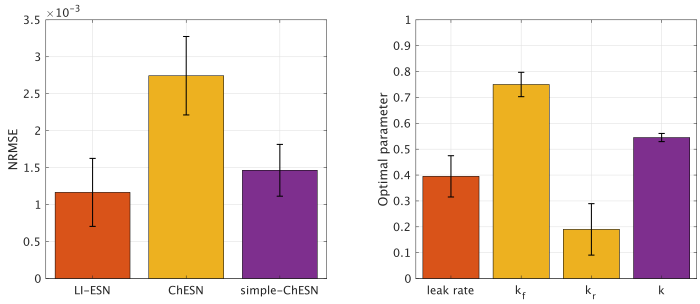

(b) Rössler task

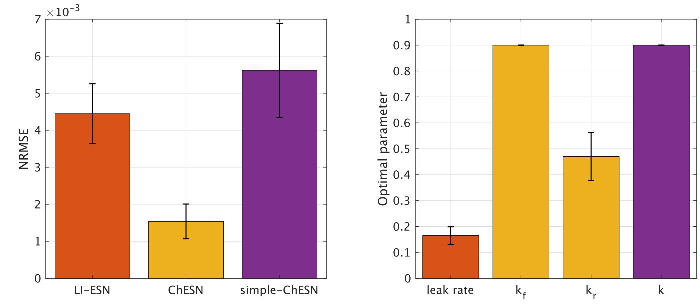

Fig. S2 Time-series prediction performance at optimal parameters obtained through grid search. The performance metric is the normalized root mean square error (NRMSE) between the target output and the predictions. The main hyperparameters affecting the performance of the reservoir in each model, namely the spectral radius and input scaling, are set to values that minimize the average NRMSE across 10 trials with varying seed values. For LI-ESN, ChESN and simple-ChESN, the spectral radius and input scale are fixed at the optimal values, and the time-history term that yielded the lowest NRMSE for each seed value is adopted (i.e., α_l in LI-ESN, k_f, k_r in ChESN, k in simple-ChESN). For simplicity, some parameters of ChESN are fixed without grid search ($k_e = 0$, $\alpha = 0.9$, $\theta = 0$). Error bars represent the standard deviation across the 10 trials.

Fig. S2, using the same method as Fig. 3 in the main text, shows the time-series prediction performance of the reservoir. From this figure, it is evident that simple-ChESN, while not matching, exhibits similar performance values to LI-ESN. Moreover, when comparing simple-ChESN with ChESN, simple-ChESN outperformed in the Lorenz task.

The reason for the inferior performance of simple-ChESN compared to LI-ESN is considered as follows. This performance difference is understood to stem from the different application of time-history terms. Unlike LI-ESN, simple-ChESN has decay coefficients in the neuron's internal state, making it more prone to values greater than 1 or less than -1, leading to saturation in the reservoir's firing state due to the tanh activation function. This saturation likely had a negative impact on performance.

Next, we explore the performance difference between simple-ChESN and ChESN. In the Rössler task, ChESN performed better. This result seems obvious given that simple-ChESN adjusts only k, whereas ChESN adjusts both k_f and k_r. However, despite such differences in the number of adjustment parameters, simple-ChESN outperformed ChESN in the Lorenz task. This could be attributed to the difference in the refractory scaling parameter ($\alpha = 0$ in simple-ChESN, $\alpha = 0.9$ in ChESN). The setting of $\alpha = 0.9$ was adopted from our previous study, which achieved high performance in Mackey-Glass time series prediction [6]. The Mackey-Glass time series used then, generated with a time delay term $\tau = 32$, exhibited a slow timescale, similar to the Rössler task in this study. This suggests that a higher α may be necessary for slow timescale time series data.

References

[1] Parker, T.S., Chua, L.: Practical Numerical Algorithms for Chaotic Systems. Springer, New York (2012). https://books.google.co.jp/books?id=lHDjBwAAQBAJ

[2] Carroll, T.L.: Do reservoir computers work best at the edge of chaos? Chaos: An Interdisciplinary Journal of Nonlinear Science **30**(12), 121109 (2020) https://doi.org/10.1063/5.0038163 . Publisher: American Institute of Physics. Accessed 2022-05-23

[3] Carroll, T.L., Pecora, L.M.: Network structure effects in reservoir computers. Chaos: An Interdisciplinary Journal of Nonlinear Science **29**(8), 083130 (2019) https://doi.org/10.1063/1.5097686 . Accessed 2022-08-13

[4] Lymburn, T., Khor, A., Stemler, T., Corrêa, D.C., Small, M., Jüngling, T.: Consistency in echo-state networks. Chaos: An Interdisciplinary Journal of Nonlinear Science **29**(2), 023118 (2019). Publisher: AIP Publishing LLC

[5] Jüngling, T., Lymburn, T., Small, M.: Consistency Hierarchy of Reservoir Computers. IEEE Transactions on Neural Networks and Learning Systems **33**(6), 2586–2595 (2022) https://doi.org/10.1109/TNNLS.2021.3119548 . Conference Name: IEEE Transactions on Neural Networks and Learning Systems

[6] Ebato, Y., Nobukawa, S., Nishimura, H.: Effect of Neural Decay Factors on Prediction Performance in Chaotic Echo State Networks. In: 2021 IEEE International Conference on Systems, Man, and Cybernetics (SMC), pp. 1888–1893 (2021). https://doi.org/10.1109/SMC52423.2021.9659012 . ISSN: 2577-1655